European Journal of Radiology Open 9 (2022) 100450

Contents lists available at ScienceDirect

European Journal of Radiology Open

journal homepage: www.elsevier.com/locate/ejro

Original article

Motion-robust MR imaging of the shoulder using compressed SENSE MultiVane

Mamoru Niitsu [a,*], Shinji Saruya [a], Katsunobu Sakaguchi [b], Keisuke Watarai [b], Masami Yoneyama [c], Yasutomo Katsumata [c], Kaiji Inoue [a], Eito Kozawa [a]

[a] Department of Radiology, Saitama Medical University, 38 Morohongo, Moroyama, Saitama 350-0495, Japan
[b] Department of Orthopedic Surgery, Saitama Medical University, 38 Morohongo, Moroyama, Saitama 350-0495, Japan
[c] Philips Japan, 2-13-37 Konan, Minato-ku, Tokyo 108-8507, Japan

HIGHLIGHTS

- Compressed SENSE (C-SENSE), an acceleration technique that combines compressed sensing with SENSE, is described.
- Combining C-SENSE with MultiVane increases motion robustness and achieves comparable scan times to Cartesian scans.
- C-SENSE MultiVane maintains image quality and is useful for MRI of the shoulder joint.

ARTICLE INFO

Keywords:
Magnetic resonance imaging
Motion artifact
Shoulder joint
Compressed SENSE
MultiVane

ABSTRACT

Purpose: Motion artifacts caused by breathing or involuntary motion of patients, which may lead to reduced image quality and a loss of diagnostic information, are a major problem in shoulder magnetic resonance imaging (MRI). The MultiVane (MV) technique decreases motion artifacts; however, it tends to prolong the acquisition time. As a parallel imaging technique, SENSitivity Encoding (SENSE) can be combined with the compressed sensing method to produce compressed SENSE (C-SENSE), resulting in a markedly reduced acquisition time. This study aimed to evaluate the use of C-SENSE MV for MRI of the shoulder joint.

Methods: Thirty-one patients who were scheduled to undergo MRI of the shoulder were included. This prospective study was approved by our institution's medical ethics committee, and written informed consent was obtained from all 31 patients. Two sets of oblique coronal images derived from the standard protocol were acquired without (standard) or with C-SENSE MV: proton-density weighted imaging (PDWI), PDWI with C-SENSE MV, T2-weighted imaging (T2WI) with fat suppression (fs), and T2WI fs with C-SENSE MV. Two radiologists graded motion artifacts and the detectability of anatomical shoulder structures on a 4-point scale (3, no artifacts/excellent delineation; 0, severe artifacts/difficulty with delineation). The Wilcoxon signed-rank test was used to compare the data for the standard and C-SENSE MV images.

Results: Motion artifacts were significantly reduced on the C-SENSE MV images ($p < 0.001$). Regarding the detectability of anatomical structures, the ratings for the C-SENSE MV sequences were significantly better ($p < 0.001$).

In conclusion, in shoulder MRI the newly developed C-SENSE MV technique reduces motion artifacts and increases the detectability of anatomical structures compared with standard sequences.

Abbreviations: MRI, magnetic resonance imaging; TSE, turbo spin echo; PDWI, proton density-weighted imaging; T2WI, T2-weighted imaging; ROI, region of interest; PI, parallel imaging; SENSE, SENSitivity Encoding; CS, compressed sensing; C-SENSE, compressed SENSE; MV, MultiVane; PROPELLER, periodically rotated overlapping parallel lines with enhanced reconstruction; BMI, body mass index; FOV, field-of-view; TE, echo time; SNR, signal-to-noise ratio; TR, repetition time; SPIR, spectral presaturation with inversion recovery; fs, fat suppression.

* Corresponding author.
E-mail address: niitsu.mamoru@1972.saitama-med.ac.jp (M. Niitsu).

https://doi.org/10.1016/j.ejro.2022.100450
Received 26 July 2022; Received in revised form 20 October 2022; Accepted 1 November 2022

1. Introduction

In magnetic resonance imaging (MRI) of the shoulder joint, motion artifacts caused by breathing or involuntary motion of patients can have important effects on the quality and diagnostic value of images. Ghosting and blurring are the main manifestations of these motion artifacts when data in the k-space are acquired in a Cartesian fashion. In standard (Cartesian) turbo spin echo (TSE) sampling, the data in the center of the k-space are acquired once or averaged. However, the data in the center of the k-space have important effects on image characteristics, and object motion can severely affect image quality. Cartesian sampling of the k-space is conducted in most clinical MRI.

The MultiVane (MV) technique is an alternative motion-robust k-space data acquisition sequence. Sequences based on the MV technique have been labelled with various acronyms by manufacturers, including periodically rotated overlapping parallel lines with enhanced reconstruction (PROPELLER), BLADE, JET, and the radial acquisition regime (RADAR). MV sequences are based on a radial k-space sampling concept, in which parallel data lines (blades) rotate around the center of the k-space, which allows spatial inconsistencies to be corrected. Data that indicate through-plane motion based on correlation measurements are rejected. Motion artifacts are further reduced through averaging at low spatial frequencies. The MV method is used extensively to reduce motion artifacts as a motion-robust scanning technique [1–10]. It has also been employed for shoulder joint MRI [11,12].

However, the MV technique has some limitations. For example, it causes streak artifacts, which affect imaging diagnosis to some extent [12]. In addition, it employs a circular shutter field-of-view (FOV), which prevents information from the four corners of the conventional square FOV from being utilized. Moreover, as it requires a high number of blades to fill the entire k-space and provide a basis for motion correction, the MV technique involves a longer scan time than Cartesian scans. Previous studies have reported that the acquisition times of MV sequences are prolonged by about 30–60% in comparison with standard Cartesian TSE sequences [4,10,13]. Thus, there is considerable interest in shortening the scan time of MV TSE sequences.

Parallel imaging (PI) has been introduced as an accelerated scanning technique to shorten scan times. To reduce the amount of acquired k-space data, in SENSitivity Encoding (SENSE), a PI method, the spatial sensitivity of each receiver in a multi-coil array is used to reconstruct MR images from undersampled k-space data, and this technique is routinely used in clinical MRI [14].

Compressed sensing (CS) is another acceleration technique involving undersampled k-space data, which exploits the sparsity in MR images to reconstruct them, thus enabling accelerated MRI acquisition [15]. CS is a signal-processing technique based on the fact that signals contain redundant information. It is used to reconstruct full images from severely undersampled k-space data while maintaining equivalent image quality. The CS method has recently been shown to result in significantly accelerated data acquisition and has been utilized in a variety of clinical MRI settings [16,17].

These accelerated scan methods, SENSE and CS, may be combined to further reduce scan times, a technique hereafter referred to as compressed SENSE (C-SENSE) [18]. C-SENSE allows scan times to be reduced and spatial image resolution to be increased. This acceleration technique shortens both single MRI sequences and full MRI examinations [19,20].

PI-accelerated MV (PROPELLER and BLADE) sequences have been reported to reduce image artifacts and produce better quality images by increasing the k-space coverage in MRI of the upper abdomen [21]. Recently, Sartoretti reported that the implementation of MV with C-SENSE is feasible and shortens scan times in rapid T2-weighted imaging (T2WI) TSE imaging of the brain [22].

This study aims to evaluate whether combining C-SENSE with MV can increase motion robustness while maintaining image quality in order to increase the clinical feasibility of shoulder joint MRI.

2. Materials and methods

This prospective study was approved by the medical ethics committee of our institution (approval number: 19058.01), and written informed consent was obtained from all of the enrolled patients. Two authors (M.Y., Y.K.) were employees of Philips Healthcare and provided technical support during the sequence development; however, they were not involved in the study design or interpretation of the data.

2.1. Patients

Forty-five patients were examined MRI of the shoulder during the period from August 2021 until January 2022. Patients who did not deliver the written informed consents or could not finish at least four sequences used for assessment were excluded. Finally, 31 patients (13 males, 18 females) were included. The indications for MRI were a suspected rotator cuff tear (n = 13), a follow-up examination after surgical rotator cuff repair (n = 13), a suspected frozen shoulder (n = 4), and suspected calcified tendinitis (n = 1). Images of 19 right and 12 left shoulders were acquired. Thirteen shoulders had undergone surgery before the MRI and been implanted with metallic devices, such as anchors. The mean patient age was 67.4 years (range, 43–79 years). The height of the patients ranged from 148.7 cm to 172.0 cm (average, 160.2 cm) and the weight of the patients ranged from 53.9 kg to 84.5 kg (average, 64.5 kg). The mean body mass index (BMI) of the patients was 25.1 (range, 20.5–29.7).

2.2. Image acquisition

All MRI examinations were performed using a 3.0-T MRI system (Ingenia Elition; Philips Healthcare, Best, the Netherlands) with an 8-channel shoulder coil. Two sets of oblique coronal images derived from the standard protocol were acquired without (standard) and with C-SENSE MV: proton density-weighted imaging (PDWI), PDWI with C-SENSE MV, T2WI with fat suppression (fs), and T2WI fs with C-SENSE MV. These four sequences were obtained in random order during the examinations of the patients. The other three sequences that are included in the standard protocol were not evaluated in this investigation: oblique sagittal PDWI fs, axial T2 * -weighted imaging, and axial T1-weighted imaging. The total examination time for each patient was approximately 25–30 min

2.3. Optimization of the C-SENSE MV sequence

The sequences were initially optimized in five healthy volunteers (Fig. 1). When the C-SENSE technique was used, the density of the blades and the number of shots per blade of the MV sequence were adjusted, and the C-SENSE reduction factor was determined. For the subjective assessment of image quality and signal-to-noise ratio (SNR) measurements, the spatial resolution including FOV, acquisition matrix, slice thickness, and slice gap, of pairs of PDWI sequences obtained with and without C-SENSE MV, and pairs of T2WI fs sequences obtained with and without C-SENSE MV were set so that they were identical. Attempts were made to ensure that the acquisition matrices of all four sequences were similar. For the fat suppression sequences, the spectral presaturation with inversion recovery (SPIR) technique was employed. The final MRI parameters of the four sequences are summarized in Table 1. The acquisition time of PDWI without and with C-SENSE MV, and T2WI fs without and with C-SENSE MV were 2 min and 41 s (2:41), 2:35, 2:26, and 2:26, respectively.

2.4. Image analysis

2.4.1. Subjective assessment of image quality

After a training session involving five cases that were not included in the analysis, two board-certified musculoskeletal radiologists, one with

Fig. 1. Optimization of the compressed SENSE MultiVane (C-SENSE MV) sequence Oblique coronal magnetic resonance (MR) images of the right shoulder of a healthy volunteer. (a) T2-weighted imaging (T2WI) with fat suppression (fs) with an acquisition time (AT) of 2:26, (b) T2WI fs MV imaging with an AT of 2:25, and (c) T2WI fs C-SENSE MV imaging with an AT of 2:26. The T2WI fs image includes a motion artifact around the humeral head (arrows, a). The T2WI fs MV image was confined by the circular shutter (arrows, b) and appears to be noisy throughout. The T2WI fs with C-SENSE MV image (c) was not obtained with a circular shutter and exhibits improved overall image quality with reduced motion artifacts. T2fs: T2WI with fat suppression, CSMV: Compressed SENSE MultiVane.

Table 1
MRI parameters of the four sequences.

	PDWI	PDWI-CSMV	T2WI fs	T2WI fs-CSMV
Sequence	Turbo Spin Echo	Turbo Spin Echo	Turbo Spin Echo	Turbo Spin Echo
FOV (mm)	140 * 140	140 * 140	140 * 140	140 * 140
Acquisition matrix	368 * 275	312 * 312	292 * 228	256 * 256
Reconstruction matrix	704 * 704	640 * 640	720 * 720	512 * 512
Slice thickness (mm)	3	3	3	3
Slice gap (mm)	0.3	0.3	0.3	0.3
Phase encoding	FH	FH	FH	FH
Oversampling (mm)	70 FH	30 FH & AP	70 FH	30 FH & AP
Bandwidth (Hz/pixel)	232	436	336	306
TR (ms)	1645	1645	2800	2800
TE (ms)	20	20	68	68
Echo-train length	12	12	19	19
DRIVE	–	–	+	+
Density of blades	–	250	–	260
Number of shots per blade	–	2	–	1
Fat suppression	–	–	SPIR	SPIR
C-SENSE reduction factor	–	2	–	2
NSA	1	1	1	1
Acquisition time (min:s)	2:41	2:35	2:26	2:26

34 years of experience, one with 17 years. evaluated the motion artifacts of the MR images and the detectability of anatomical structures on the MR images and attempted to reach a consensus regarding their findings. The readers were unaware of the specific sequence used and the patient's clinical data. A four-grade classification system for motion artifacts was used: 3, no motion artifacts; 2, minimal motion artifacts; 1, moderate motion artifacts; and 0, severe motion artifacts or not diagnostically usable. A four-grade classification system was also used to assess the detectability of anatomical shoulder structures (the rotator cuff, the glenoid labrum, the articular cartilage, the internal structures of the bones, and the joint capsules and surrounding bursae): 3, excellent delineation of the abovementioned structures; 2, good delineation and minor diagnostic impairment; 1, poor delineation and diagnostic possibilities limited to major findings; and 0, difficulty in delineation and detection.

2.4.2. Statistical analyses

The scores for motion artifacts and the detectability of anatomical structures were averaged separately for each sequence. All statistical analyses were performed using JMP software v16 (SAS Institute, Cary, NC, USA). The non-parametric Wilcoxon signed-rank test was used to compare the standard and C-SENSE MV sequences with respect to the readers' assessments of motion artifacts and the detectability of anatomical structures. All p-values of < 0.05 were considered to be statistically significant.

3. Results

Motion artifacts were significantly reduced in the C-SENSE MV sequences compared with standard TSE imaging. The standard TSE images obtained with PDWI and T2WI fs frequently suffered from motion artifacts. Linear or concave high- and/or low-intensity stripes were superimposed onto the TSE images, and these artifacts were sometimes severe or indistinct, depending on the physical condition of the patient. Due to this noisy appearance, the overall quality of these images was reduced. The detectability of normal morphologies and pathologies of the shoulder joint, including cuff tears and thickened synovial pouches, was impaired (Fig. 2).

In some cases, in which no motion artifacts were recognized on the images obtained with or without C-SENSE MV, the grades for motion artifacts and the detectability of anatomical structures were evaluated to be equivalent (Fig. 3). For post-surgical shoulders, delineation of the repaired rotator cuff was sometimes adversely affected by motion artifacts around the joint (Fig. 4).

In the subjective assessments of motion artifacts and the detectability of anatomical structures, the mean motion artifact scores of the PDWI and PDWI C-SENSE MV sequences were 1.87 and 2.58, respectively ($p < 0.001$). The mean motion artifact scores of the T2WI fs and T2WI fs C-SENSE MV sequences were 1.55 and 2.52, respectively ($p < 0.001$). The mean anatomical structure detectability scores of the PDWI and PDWI C-SENSE MV sequences were 2.16 and 2.48, respectively ($p < 0.001$), and those of the T2WI fs and T2WI fs C-SENSE MV sequences were 1.68 and 2.39, respectively ($p < 0.001$) (Fig. 5).

4. Discussion

Among the various joints subjected to MRI, the shoulder joint is the most vulnerable to motion artifacts [23]. If the patient moves when the center of the k-space is being acquired during a Cartesian scan, which determines the image contrast, it may result in bulky motion artifacts.

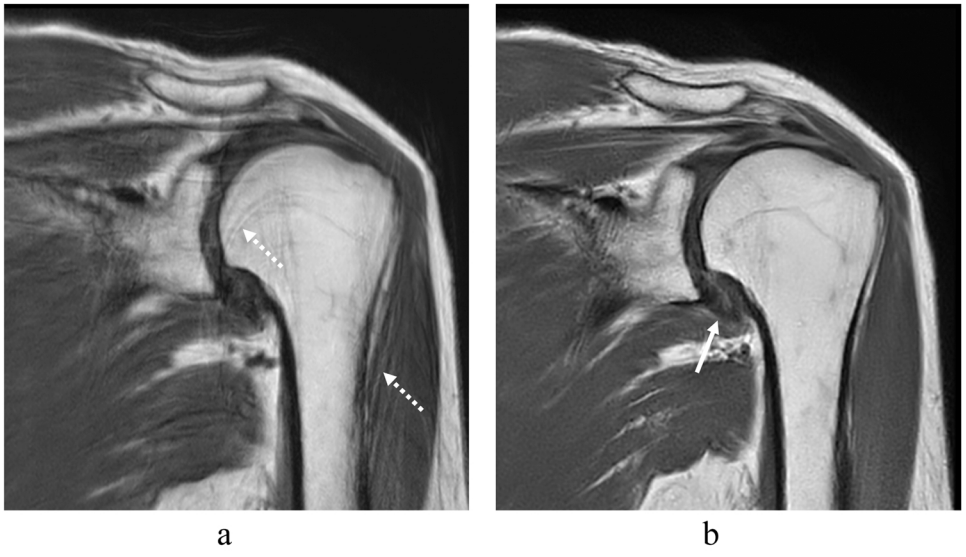

Fig. 2. Oblique coronal (a) proton density-weighted imaging (PDWI), (b) PDWI C-SENSE MV, (c) T2WI fs, and (d) T2WI fs C-SENSE MV images of the left shoulder of a 74-year-old female with a suspected rotator cuff tear On the standard images (a and c), some motion artifacts are covering anatomical structures (dashed arrows, a and c), reducing the overall image quality. When C-SENSE MV was used, the motion artifacts were partially reduced; however, some artifacts remained (b and d). The C-SENSE MV images show improved delineation of the thickened axillary pouch (arrow, b) and the intratendinous cleft in the supraspinatus tendon (arrow, d). In the subjective assessment of the images, the following motion artifact grades were obtained: PDWI: 0 (a), PDWI C-SENSE MV: 2 (b), T2WI fs: 0 (c), and T2WI fs C-SENSE MV: 1 (d) (PDWI: 0–2, T2fs: 0–1). The detectability grades were as follows: PDWI: 0–2, T2fs: 0–2.

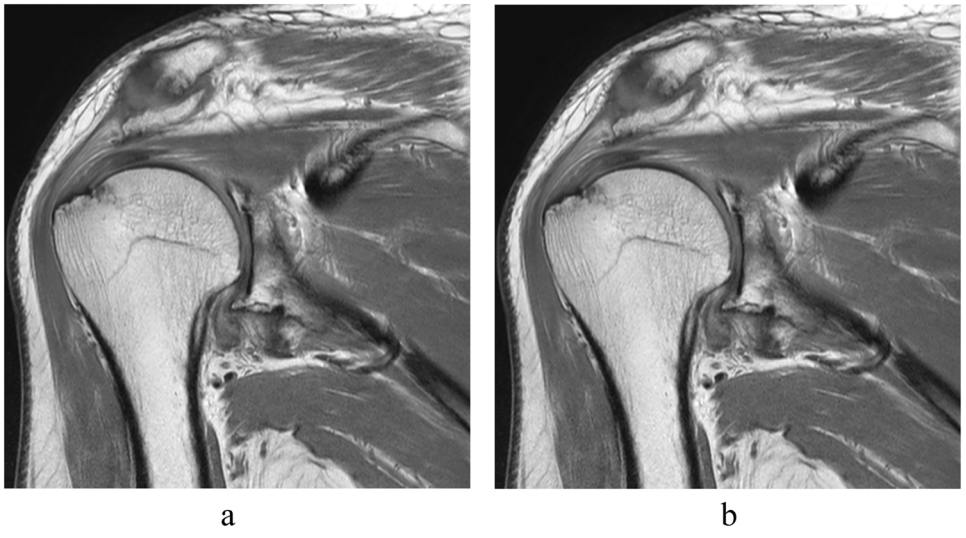

Fig. 3. Oblique coronal (a) PDWI and (b) PDWI C-SENSE MV images of the right shoulder of a 79-year-old male with a suspected rotator cuff tear. No significant motion artifacts can be seen on the standard or C-SENSE MV images. Fine structures, including the supraspinatus tendon; the glenoid fossa, which exhibits spur formation; the internal bony texture of the humerus; and the belly of the subscapularis muscle, are precisely delineated on both types of images. The following motion artifact grades were obtained: PDWI: 3 (a), PDWI C-SENSE MV: 3 (b) (PDWI: 3–3). The following detectability grades were obtained: PDWI: 3–3.

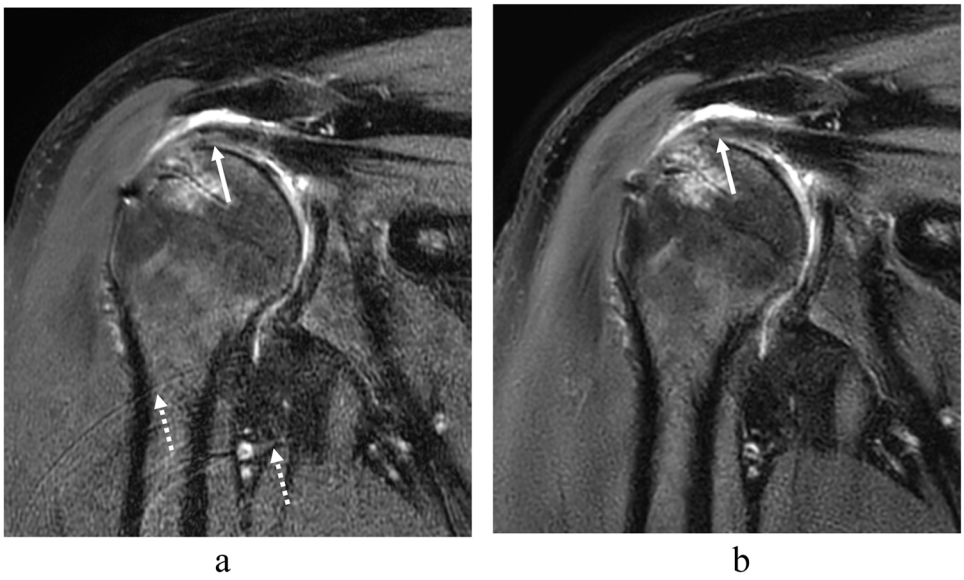

Fig. 4. Oblique coronal (a) T2WI fs and (b) T2WI fs C-SENSE MV images of the right shoulder of a 79-year-old male after rotator cuff repair. Minimal motion artifacts can be seen on the standard images (dashed arrows, a). The repaired supraspinatus tendon, which exhibits minor irregularities, is shown on both types of images (arrows, a and b). The following motion artifact grades were obtained: T2fs: 2 (a), T2WI fs C-SENSE MV: 3 (b) (T2fs: 2–3). The following detectability grades were obtained: T2fs: 2–2.

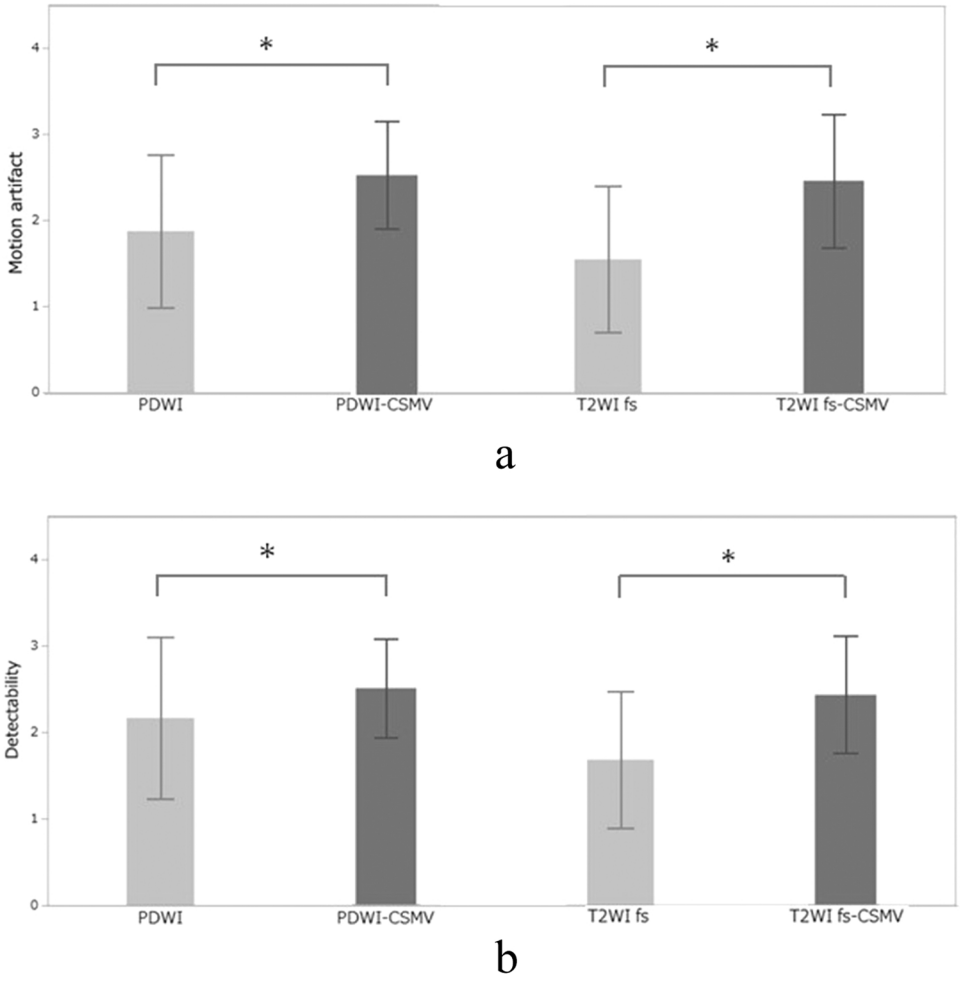

Fig. 5. Gray bar graphs of the motion artifact (a) and anatomical detectability (b) scores. The PDWI C-SENSE MV sequence was significantly superior to the PDWI sequence with regard to the level of motion artifacts ($p < 0.001$) (a) and with regard to the detectability of anatomical structures ($p < 0.001$) (b). The T2WI fs C-SENSE MV sequence was significantly superior to the T2WI fs sequence with regard to the level of artifacts ($p < 0.001$) (a) and the detectability of anatomical structures ($p < 0.001$) (b). CSMV: Compressed SENSE MultiVane; *$p < 0.05$, statistically significant.

There may be technical improvement strategy, including adjustment of the phase encoding direction and saturation-bands placement, however, to our experience, they cannot suppress the motion artifacts satisfactorily. For example, severe motion artifact evoked by patients with pain, remained even after every efforts including technical adjustment mentioned above. And if enlarged synovial bursae or synovial cyst adjacent to shoulder joint exist, effect of the saturation-bands was limited. Thus, motion artifacts are a major concern in shoulder MRI.

Another reason that deteriorates the imaging quality of the shoulder MRI includes the patient's dimension; height and weight. In our patient

population, the max height was 172.0 cm and the max weight was 84.5 kg. No patient complaint of the narrowness within the magnet bore or sign of claustrophobia. Moreover, the size of the shoulder seems to be crucial for image quality, because the position of shoulder within the bore may determine effectiveness of the fat suppression and susceptibility artifacts. We made every effort to place the examining shoulder as close as possible to the center line of the bore and to hold the shoulder within the shoulder coil that the patient feels comfortable enough to stay still.

The MV sequence is an alternative k-space data acquisition method to the standard (Cartesian) sampling method and is widely used to reduce motion artifacts, as it is a motion-robust technique. In this k-space sampling scheme, multiple echo trains of a TSE sequence are acquired in a rotating partially overlapping fashion. In addition, k-space data are acquired for the central region and averaged. Furthermore, the center of the k-space is oversampled, which reduces the sequence's susceptibility to artifacts [3,13]. To provide a basis for motion correction, it requires a large number of blades to fill the entire k-space, and this leads to longer scan times compared with Cartesian scans. Theoretically, to maintain an equivalent spatial resolution, data oversampling in the central region of the k-space requires the imaging time to be increased by a factor of $\pi/2$ compared with standard MRI [13]. This is one reason that we set smaller acquisition matrix for the C-SENSE MV imaging than that used for the standard imaging (to be stated later in the limitation section).

By combining the C-SENSE technique with the MV sequence, the acquisition time can be reduced to a similar length to that seen in standard imaging, while motion artifacts are reduced and image quality is maintained. The conventional MV sequence employs a circular shutter FOV; however, combining the C-SENSE technique with the MV sequence could reduce the acquisition time without using a circular shutter. Streak artifacts, which are artifacts caused by undersampling that are specific to the MV sequence, are generated when trying to reduce the scan time. In this study, no marked streak artifacts were observed when the C-SENSE MV sequence was used. Such streak artifacts were minimized by the use of both PI (having data redundancy because of the use of multiple receiver coil channels) and the compressed sensing technology (information redundancy). This approach reduced streak artifacts caused by undersampling, but it may not have removed those caused by data inconsistency, e.g., due to motion. Fundamentally, streak artifacts may be mixed with motion artifacts, and it is challenging to distinguish them from motion artifacts.

Our study had some limitations. First, the acquisition matrix and the reconstruction matrix for the C-SENSE MV imaging was smaller than that used for the standard imaging. In the MV technique, sparse scanning of the peripheral regions of the k-space results in a comparatively small acquisition matrix (large voxels). Regarding signal-to-noise ratio (SNR), larger voxels can be beneficial in C-SENSE MV imaging. Previous studies have reported that redundant data sampling in the PROPELLER technique increases the SNR [13] and in sagittal T2WI BLADE imaging of the cervical spine the SNR of the vertebral body and spinal cord were significantly higher than those seen with the standard TSE sequence [24]. In the subjective assessment of image quality, both the motion artifact and anatomical detectability scores of the C-SENSE MV sequences were much higher than those of the standard sequence. Second, we only evaluated the clinical usefulness of C-SENSE MV on oblique coronal PDWI and T2WI fs images, and other routine clinical sequences, including oblique sagittal PDWI fs, axial T2 * -weighted images, and axial T1-weighted images, were not evaluated in this study because we considered that oblique coronal PDWI and T2WI fs images are the most motion-sensitive and clinically important images, and hence, we focused on whether C-SENSE MV improves the quality of these images. Nevertheless, other sequences, including the T2 * gradient echo sequence can also be combined with C-SENSE MV [25], and we believe that C-SENSE MV also helps to improve the motion robustness of these sequences while maintaining sufficient image contrast and without prolonging the acquisition time. Third, we assessed the image quality by subjective, four-grade classification system alone. Initially, in addition to the subjective, qualitative method, we attempted to measure SNR. However, SNR measurement in PI and CS is still controversial. The signal and noise levels in reconstructed images principally depend on the sensitivity profiles of the receiver coils and are influenced by the acceleration factors of the PI. CS is an iterative process performed on k-space when the signal acquisition has been performed. For these reasons, we abandoned quantitative analysis using SNR measurement. Lastly, we set higher value of the bandwidth (BW) in the PDWI C-SENSE MV sequences than the standard imaging. Higher BW may influence the overall image quality including SNR and image sharpness, however, it can suppress chemical shift artifact from the fatty tissue in PDWI. In contrast, fat signals were fundamentally suppressed in the fat suppression T2WI, we set lower BW in the T2WI fs C-SENSE MV sequence.

5. Conclusions

Using non-Cartesian sampling schemes, the newly developed C-SENSE MV technique can be used to produce motion robust sequences, which increases the clinical feasibility of shoulder joint MRI. Actually we have implemented new sequences into dairy clinical practice.

Ethical approval

Institutional review board approval was obtained.

Funding

This research did not receive any specific grants from funding agencies in the public, commercial, or not-for-profit sectors.

CRediT authorship contribution statement

Mamoru Niitsu: Investigation, Writing – original draft; Saruya Shinji: Resources, Data curation; Katsunobu Sakaguchi: Resources, Data curation; Keisuke Watarai: Resources, Data curation; Masami Yoneyama: Sequence development; Yasutomo Katsumata: Sequence development; Kaiji Inoue: Writing – statistics & editing; Eito Kozawa: Supervision, Project administration.

Declaration of Competing Interest

Two of the authors (M.Y., Y.K.) are employees of Philips Japan. The other authors declare that they have no known competing financial interests or personal relationships that could have appeared to influence this study.

Acknowledgement

The authors thank Dr. Michio Shiibashi for his help with statistical work.

References

[1] Y. Hirokawa, H. Isoda, Y.S. Maetani, S. Arizono, K. Shimada, K. Togashi, MRI artifact reduction and quality improvement in the upper abdomen with PROPELLER and prospective acquisition correction (PACE) technique, AJR Am. J. Roentgenol. 191 (2008) 1154–1158, http://doi: 10.2214/AJR.07.3657.

[2] H.J. Michaely, H. Kramer, S. Weckbach, O. Dietrich, M.F. Reiser, S.O. Schoenberg, Renal T2-weighted turbo-spin-echo imaging with BLADE at 3.0 Tesla: initial experience, J. Magn. Reson. Imaging 27 (2008) 148–153, https://doi.org/10.1002/jmri.21240.

[3] Y. Ohgiya, J. Suyama, N. Seino, S. Takaya, M. Kawahara, M. Saiki, S. Sai, M. Hirose, T. Gokan, MRI of the neck at 3 Tesla using the periodically rotated overlapping parallel lines with enhanced reconstruction (PROPELLER) (BLADE) sequence compared with T2-weighted fast spin-echo sequence, J. Magn. Reson. Imaging 32 (2010) 1061–1067, https://doi.org/10.1002/jmri.22234.

[4] A.B. Rosenkrantz, L. Mannelli, D. Mossa, J.S. Babb, Breath-hold T2-weighted MRI of the liver at 3T using the BLADE technique: impact upon image quality and lesion detection, Clin. Radiol. 66 (2011) 426–433, https://doi.org/10.1016/j.crad.2010.10.018.

[5] E. Lavdas, P. Mavroidis, S. Kostopoulos, D. Glotsos, V. Roka, T. Topalzikis, A. Bakas, G. Oikonomou, N. Papanikolaou, G. Batsikas, I. Kaffes, D. Kechagias, Improvement of image quality using BLADE sequences in brain MRI imaging, Magn. Reson Imaging 31 (2013) 189–200, https://doi.org/10.1016/j.mri.2012.08.001.

[6] J.H. Lee, Y.H. Choi, J.E. Cheon, S.M. Lee, H.H. Cho, S.M. Shin, W.S. Kim, I.O. Kim, Improved abdominal MRI in non-breath-holding children using a radial k-space sampling technique, Pedia Radio. 45 (2015) 840–846, https://doi.org/10.1007/s00247-014-3244-1.

[7] S. Bayramoglu, O. Kilickesmez, T. Cimilli, A. Kayhan, G. Yirik, F. Islim, S. Alibek, T2-weighted MRI of the upper abdomen: comparison of four fat-suppressed T2-weighted sequences including PROPELLER (BLADE) technique, Acad. Radiol. 17 (2010) 368–374, https://doi.org/10.1016/j.acra.2009.10.015.

[8] T. Finkenzeller, C.M. Wendl, S. Lenhart, C. Stroszczynski, G. Schuierer, C. Fellner, BLADE sequences in transverse T2-weighted MR imaging of the cervical spine. cut-off for artefacts? Rofo 36 (2015) 102–108, https://doi.org/10.1055/s-0034-1385179. PMID: 25912327 Review.

[9] T. Kojima, H. Yabuuchi, H. Narita, S. Kumazawa, Y. Yamasaki, Y. Yano, N. Sakai, Y. Kurihara, K. Hisada, M. Masaki, H. Kimura, Efficacy of the radial acquisition regime (RADAR) for acquiring head and neck MR images, Br. J. Radiol. 89 (2016) 89, https://doi.org/10.1259/bjr.20160007.

[10] P. Mavroidis, E. Giankou, A. Tsikrika, E. Kapsalaki, V. Chatzigeorgiou, G. Batsikas, G. Zaimis, S. Kostopoulos, D. Glotsos, K. Ninos, V. Georgountzos, D. Kavouras, E. Lavdas, Brain imaging: comparison of T1W FLAIR BLADE with conventional T1W SE, Magn. Reson Imaging 37 (2017) 234–242, https://doi.org/10.1016/j.mri.2016.12.007.

[11] T.J. Dietrich, E.J. Ulbrich, M. Zanetti, S.F. Fucentese, C.W. Pfirrmann, PROPELLER technique to improve image quality of MRI of the shoulder, AJR Am. J. Roentgenol. 197 (2011) W1093–W1100, https://doi.org/10.2214/AJR.10.6065.

[12] K. Nagatomo, H. Yabuuchi, Y. Yamasaki, H. Narita, S. Kumazawa, T. Kojima, N. Sakai, M. Masaki, H. Kimura, Efficacy of periodically rotated overlapping parallel lines with enhanced reconstruction (PROPELLER) for shoulder magnetic resonance (MR) imaging, Eur. J. Radiol. 85 (10) (2016) 1735–1743, https://doi.org/10.1016/j.ejrad.2016.07.008.

[13] J.G. Pipe, Motion correction with PROPELLER MRI: application to head motion and free-breathing cardiac imaging, Magn. Reson. Med. 42 (1999) 963–969, https://doi.org/10.1002/(sici)1522-2594(199911)42:5<963::aid-mrm17>3.0.co.

[14] K.P. Pruessmann, M. Weiger, M.B. Scheidegger, P. Boesiger, SENSE: sensitivity encoding for fast MRI, Magn. Reson Med. 42 (1999) 952–962, https://doi.org/10.1002/(sici)1522-2594(199911)42:5<952::aid-mrm16>3.0.co;2-s.

[15] M. Lustig, D. Donoho, J.M. Pauly, Sparse MRI: the application of compressed sensing for rapid MR imaging, agn Reson Med. 58 (2007) 1182–1195, https://doi.org/10.1002/mrm.21391.

[16] O.N. Jaspan, R. Fleysher, M.L. Liptin, Compressed sensing MRI: a review of the clinical literature, Br. J. Radio. 88 (2015) 20150487, https://doi.org/10.1259/bjr.20150487.

[17] J.C. Ye, Compressed sensing MRI: a review from signal processing perspective, BMC Biomed. Eng. 1 (2019) 8–25, https://doi.org/10.1186/s42490-019-0006-z.

[18] L. Geerts-Ossevoort, E. deWeerdt, A. Duijndam, G. van Ijperen, H. Peeters, M.. Doneva, M. Nijenhuis, A. Huang, Compressed SENSE. Speed done right. Every time. (2018) Available via https://philipsproductcontent.blob.core.windows.net/assets/20180109/619119731f2a42c4acd4a863008a46c7.pdf.

[19] Y. Ma, Y. Hou, Q. Ma, X. Wang, S. Sui, B. Wang, Compressed SENSE single-breath-hold and free-breathing cine imaging for accelerated clinical evaluation of the left ventricle, 325-325, Clin. Radiol. 74 (2019), https://doi.org/10.1016/j.crad.2018.12.012.

[20] M. Kocaoglu, A.S. Pednekar, H. Wang, T. Alsaied, M.D. Taylor, M.S. Rattan, Breath-hold and free-breathing quantitative assessment of biventricular volume and function using compressed SENSE: a clinical validation in children and young adults, J. Cardiovasc Magn. Reson 22 (2020) 54, https://doi.org/10.1186/s12968-020-00642-y.

[21] Y. Hirokawa, H. Isoda, Y.S. Maetani, S. Arizono, K. Shimada, K. Togashi, Evaluation of motion correction effect and image quality with the periodically rotated overlapping parallel lines with enhanced reconstruction (PROPELLER) (BLADE) and parallel imaging acquisition technique in the upper abdomen, J. Magn. Reson Imaging 28 (2008) 957–962, https://doi.org/10.1002/jmri.21538.

[22] E. Sartoretti, M. Wyss, B. Eichenberger, L. van Smoorenburg, C.A. Binkert, S. Sartoretti-Schefer, T. Sartoretti, Rapid T2-weighted turbo spin echo MultiVane brain MRI using compressed SENSE: a qualitative analysis, 786.e15-786.e22, Clin. Radio. 76 (2021), https://doi.org/10.1016/j.crad.2021.06.017.

[23] C.K. Goh, W.C.G. Peh, Pitfalls in magnetic resonance imaging of the shoulder, Can. Assoc. Radiol. J. 63 (2012) 247–259, https://doi.org/10.1016/j.carj.2011.02.005.

[24] C. Fellner, C. Menzel, F.A. Fellner, C. Ginthoer, N. Zorger, A. Schreyer, E.M. Jung, S. Feuerbach, T. Finkenzellera, BLADE in sagittal T2-weighted MR Imaging of the cervical spine, AJNR Am. J. Neuroradiol. 31 (2010) 674–681, https://doi.org/10.3174/ajnr.A1894. PMCID: PMC7964237 PMID: 19942708.

[25] H. Peeters, H. Chung, G. Valvano, D. Yakisikli, J. van Gemert, E. de Weerdt K. van de Ven. Philips SmartSpeed: No compromise Image quality and speed at your fingertip. (2022) Available via https://www.philips.com/c-dam/b2bhc/master/landing-pages/smartspeed/philips-smart-speed-brochure.pdf.